Contrast Agents for MRI: Recent Advances

Sophie Laurent, Luce Vander Elst and Robert N. Muller
University of Mons-Hainaut, Mons, Belgium

1 CONTRAST IN MRI – PRINCIPLES

Magnetic resonance imaging (MRI) is a noninvasive technique that allows the characterization of pathological tissues and lesions. The image results from the spatial registration of hydrogen nuclei. It is made of elements called *pixels*, the gray level of which represents the signal intensity emitted by the corresponding volume elements, *voxels*. As the signal depends on the concentration of protons and on the nuclear relaxation times, T_1 (the spin lattice or longitudinal relaxation time) and T_2 (the spin–spin or transverse relaxation time), modulations – sometimes complex – of image intensity are observed. Intensity differences between adjacent voxels determine the image contrast.[1]

Variations in the natural contrast can be achieved by modifying the instrumental or "extrinsic factors" of the imaging process, such as the parameters of the pulse acquisition sequence, or by taking advantage of the "intrinsic" parameters, such as the local concentration of the nuclei (also called ρ, the spin density), their relaxation parameters (T_1, T_2, and T_2*), their relative bulk magnetic susceptibility, the bulk flow, or their molecular self-diffusion coefficient. Such strategies allow an improvement of the image contrast.

In addition to utilizing these extrinsic and intrinsic factors, it is possible to improve contrast still further by exogenously administered contrast agents. Indeed, a precise and nonambiguous medical diagnosis can often be reached with the help of contrast agents, which facilitate the distinction between a pathological tissue and its healthy surroundings. Among the relevant characteristics of these substances, their efficiency and their safety must be assessed before considering their clinical use. The contrast agents have, therefore, to be stable, nontoxic, biocompatible, and efficient at low doses.

As mentioned earlier, the intensity of the MR signal arising from a voxel is determined by its proton concentration (also called *proton density*) and the water proton's relaxation. For instance, modification of the proton density has been used for reducing the signal of the bowel: perfluoroctylbromide (PFOB, $C_8F_{17}Br$), barium sulfate, and clays darken the bowels by decreasing the water content of the intestinal cavity. They also modify the water protons' nuclear relaxation kinetics by offering large absorption surfaces. Although relaxation parameters may be influenced by an alteration of the water molecular dynamics, they are more efficiently modified by intensifying dipole–dipole magnetic interactions.

The process of relaxation is a function of the water proton environment and varies according to the tissues. Contrast agents able to decrease T_1 usually induce an increase of the signal intensity (positive agents), while those having an effect mainly on T_2 decrease the signal intensity (negative agents). Images can thus be T_1 or T_2 weighted.

2 MODIFICATION OF THE NUCLEAR RELAXATION RATES

Theory predicts that the relaxation process of an excited proton surrounded by a magnetic center and submitted to a static field of 1.5 T will require a few seconds. For pure water solution, the longitudinal relaxation time T_1 is indeed around 4 s. In tissues, due to a slower molecular dynamics, it is around several hundred milliseconds. If an electron, which is 658 times more magnetic than a proton, is located in close vicinity of the hydrogen nucleus, the electron–nucleus interaction, which increases as the square of the magnetic moments, leads to a much faster relaxation process (a few microseconds).

Relaxation agents should thus be chemical structures rich in unpaired electrons, like organic stable free radicals, molecular oxygen, or paramagnetic metal ions. The most efficient elements are transition metal ions (Fe^{2+}, Fe^{3+}, Mn^{2+}, Mn^{3+}, etc.) or lanthanide (III) ions (Gd^{3+}, Dy^{3+}, etc.). The preferred ion for MRI applications is Gd^{3+} because of its favorable magnetic properties (seven unpaired electrons, eight coordinated water molecules, and relatively long electron spin-relaxation time). However, this ion is toxic and must be coordinated by chelating organic ligands to be usable in vivo.[2,3]

In addition, nanocrystals of iron oxide, called *superparamagnetic materials*, are known to exhibit extremely high magnetic moments at high magnetic fields and are thus drawing much interest in MRI.[4,5]

3 RELAXIVITY

The signal enhancement produced by contrast agents depends on their longitudinal r_1 or transverse r_2 relaxivities, which are defined as the increase of relaxation rates ($R_1 = 1/T_1$ and $R_2 = 1/T_2$) produced by 1 mM of magnetic center per liter (equation 1). r_1 and r_2 are expressed in per second per millimole and are characteristic of the contrast agent efficacy. The observed relaxation rate $R_{i(\mathrm{obs})}$ ($= 1/T_{i(\mathrm{obs})}$) of a water solution or a tissue is given by equation (1)

$$R_{i(\mathrm{obs})} = \frac{1}{T_{i(\mathrm{obs})}} = \frac{1}{T_{i(d)}} + \frac{1}{T_{i(p)}} = \frac{1}{T_{i(d)}} + r_i C \quad \text{with} \quad i = 1 \text{ or } 2 \tag{1}$$

where $T_{i(\mathrm{d})}$ is the relaxation time of the system before adding the contrast agent, also called the *diamagnetic contribution* (s);

eMagRes, Online © 2007 John Wiley & Sons, Ltd.

This article was previously published in the *Encyclopedia of Magnetic Resonance* in 2009 by John Wiley & Sons, Ltd.
DOI: 10.1002/9780470034590.emrstm1049

and $T_{i(p)}$, the paramagnetic relaxation time, is the relaxation time resulting from the presence of the contrast agent, which is related to C the concentration of the magnetic center (millimole per liter) and r_i the relaxivity (per second per millimole liter). The relaxivity $r_{1,2}$ is a complex function of several parameters of the molecular structure and dynamics of the contrast agent.

4 RELAXATION MECHANISMS

4.1 Paramagnetic Relaxation

A general theory of nuclear relaxation in the presence of paramagnetic substances was developed by Bloembergen, Solomon, and Freed.[6] According to this theory, paramagnetic complexes induce an increase of both the longitudinal and transverse relaxation rates, R_1 and R_2. The paramagnetic relaxation of the water protons originates from the dipole–dipole interactions between the nuclear spins and the fluctuating local magnetic fields caused by the unpaired electron spins. These magnetic fields around the metal ion decrease rapidly with distance. The water molecules that are coordinated with the metal center and the bulk solvent molecules diffusing around the metal ion both contribute to the relaxation effect. Paramagnetic relaxation can be explained by three mechanisms called the *inner sphere* (*IS*), *second sphere* (*SS*), and *outer sphere* (*OS*) contributions (equation 2, Figure 1). The IS relaxation concerns the water molecule(s) bound in the first coordination sphere of the metal ion and exchanging with the bulk solvent; the SS relaxation is related to the second coordination sphere water molecules (like hydrogen-bound molecules) exchanging quite fast with the bulk, and the OS relaxation is due to translational diffusion of the water molecules near the chelate.

$$\frac{1}{T_{i(p)}} = \left(\frac{1}{T_{i(p)}}\right)^{\mathrm{IS}} + \left(\frac{1}{T_{i(p)}}\right)^{\mathrm{SS}} + \left(\frac{1}{T_{i(p)}}\right)^{\mathrm{OS}} \qquad (2)$$

4.1.1 *Inner-sphere Mechanism*

The IS contribution is modulated by the chemical exchange of the coordinated water protons with the bulk water (residence time τ_M), the reorientation of the whole complex (rotational correlation time τ_R), and the electronic spin relaxation (electronic relaxation times τ_{s1} and τ_{s2}) (Figure 2).

The relaxation time of the water protons located in the first coordination sphere of Gd^{3+} (T_{iM}) results mainly from the dipole–dipole interaction between the nucleus and the unpaired electrons. The contribution of the IS mechanism is given by equations (3) and (4):

$$R_1^{\mathrm{IS}} = fq\frac{1}{T_{1M} + \tau_M} \qquad (3)$$

$$R_2^{\mathrm{IS}} = f.q.\frac{1}{\tau_M}\frac{T_{2M}{}^{-2} + \tau_M{}^{-1}T_{2M}{}^{-1} + \Delta\omega_M{}^2}{(\tau_M{}^{-1} + T_{2M}{}^{-1})^2 + \Delta\omega_M{}^2} \qquad (4)$$

where f is the relative concentration of the paramagnetic complex and of the water molecules, q is the number of water molecules in the first coordination sphere, τ_M is the water residence time of the water bound to the paramagnetic ion, and $\Delta\omega_M$ is the chemical shift difference between bulk and coordinated water. If $\Delta\omega_M \leq \tau_M{}^{-1}$ and $T_{2M}{}^{-1}$, equation (4) is similar to equation (3).

For paramagnetic complexes like those used in MRI, T_{1M} and T_{2M} are given by the Solomon–Bloembergen–Morgan theory (equations 5–9).

$$\frac{1}{T_{1M}} = \frac{2}{15}\left(\frac{\mu_0}{4\pi}\right)^2 \gamma_H^2\mu_B^2 g_L{}^2 J(J+1)\frac{1}{r^6} \times \left[\frac{3\tau_{c1}}{1+\omega_H^2\tau_{c1}^2} + \frac{7\tau_{c2}}{1+\omega_S^2\tau_{c2}^2}\right] \qquad (5)$$

$$\frac{1}{T_{2M}} = \frac{1}{15}\left(\frac{\mu_0}{4\pi}\right)^2 \gamma_H^2\mu_B^2 g_L{}^2 J(J+1)\frac{1}{r^6} \times \left[4\tau_{c1} + \frac{13\tau_{c2}}{1+(\omega_S\tau_{c2})^2} + \frac{3\tau_{c1}}{1+(\omega_H\tau_{c1})^2}\right] \qquad (6)$$

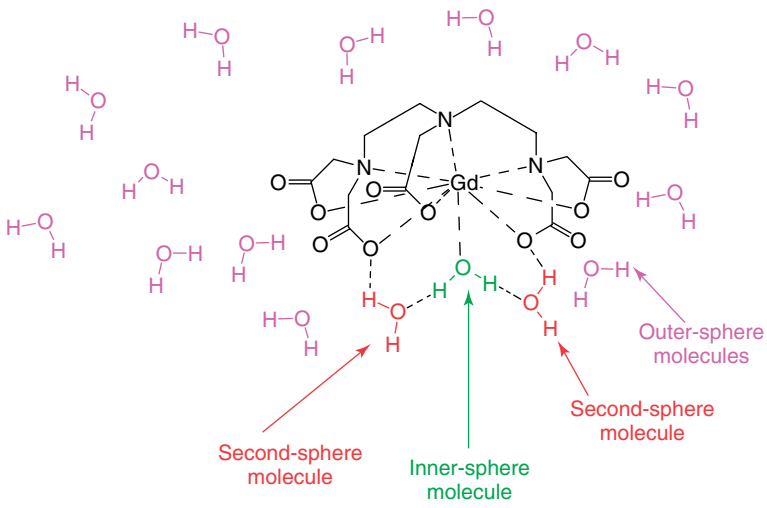

Figure 1 Paramagnetic relaxation mechanisms

eMagRes, Online © 2007 John Wiley & Sons, Ltd.
This article is © 2009 John Wiley & Sons, Ltd.
This article was previously published in the *Encyclopedia of Magnetic Resonance* in 2009 by John Wiley & Sons, Ltd.
DOI: 10.1002/9780470034590.emrstm1049

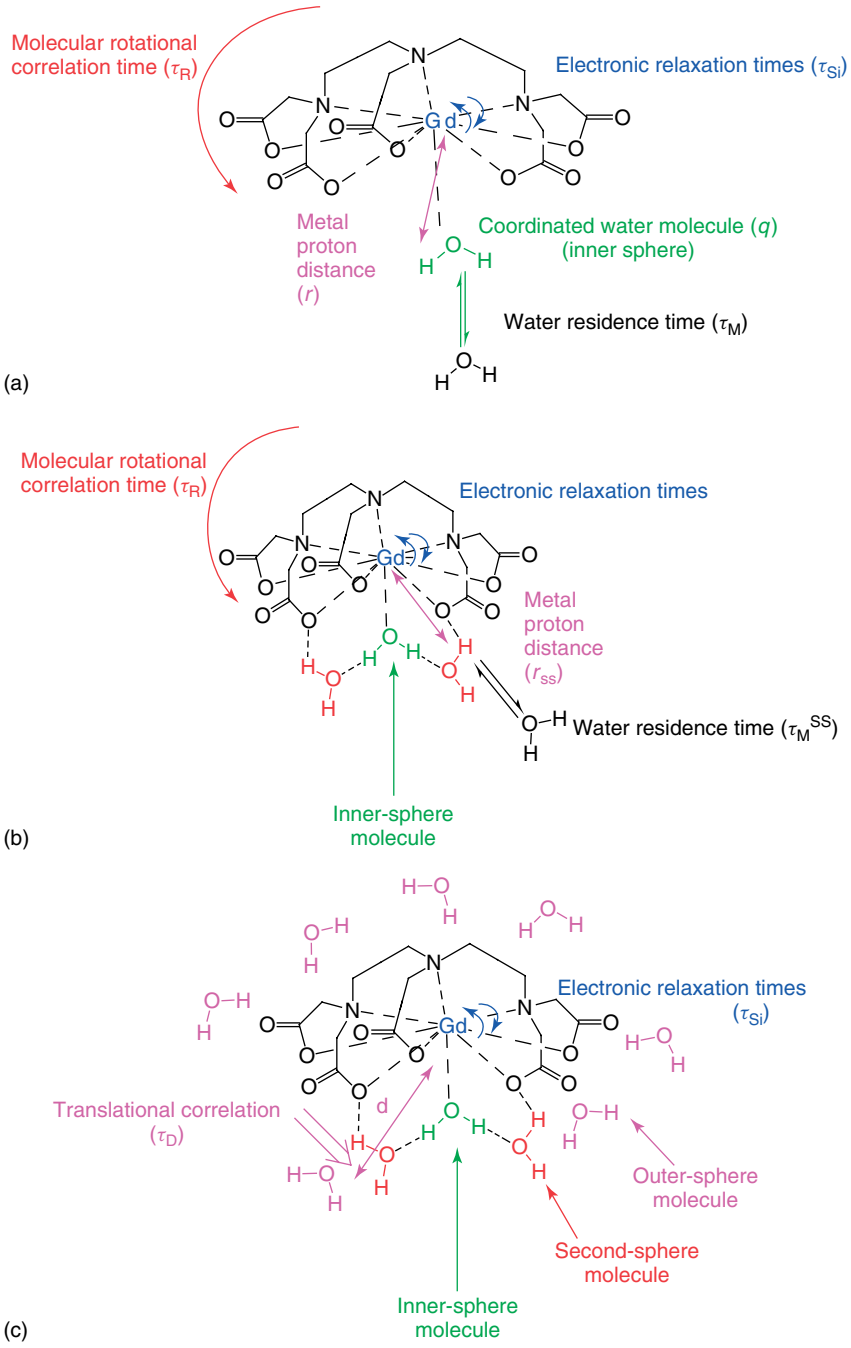

Figure 2 Inner sphere (a), second sphere (b), and outer sphere (c) mechanisms

with

$$\frac{1}{\tau_{ci}} = \frac{1}{\tau_R} + \frac{1}{\tau_M} + \frac{1}{\tau_{si}} \tag{7}$$

where

μ_0 is the permeability of the vacuum,
γ_H is the gyromagnetic ratio of the proton,
μ_B is the Bohr magneton,
g_L is the Landé factor [$g_L(Gd^{3+}) = 2.0$],
J is the total spin quantum number [$J(Gd^{3+}) = S(Gd^{3+}) = 7/2$],
$\omega_{S,H}$ is the angular frequencies of the electron and of the proton, respectively,
r is the distance between the coordinated water protons and the unpaired electron spins,
$\tau_{c1,2}$ is the correlation times modulating the interaction,
τ_R is the rotational correlation time of the hydrated complex, and
$\tau_{s1,2}$ is the longitudinal and transverse relaxation times of the electrons.

These latter parameters are field dependent and can be described by equations (8) and (9).

$$\frac{1}{\tau} = \frac{1}{5\tau} \quad \frac{1}{1 \quad \omega^{2}\tau^{2}} + \frac{4}{2 \quad 2} \tag{8}$$

DOI: 10.1002/9780470034590.emrstm1049

$$\frac{1}{\tau_{S2}} = \frac{1}{10\tau_{SO}}\left[3 + \frac{5}{1+\omega_S{}^2\tau_V{}^2} + \frac{2}{1+4\omega_S{}^2\tau_V{}^2}\right] \quad (9)$$

with τ_{sO}, the value of $\tau_{s1,2}$ at zero field and τ_v, the correlation time characteristic of the electronic relaxation times.

If Gd^{3+} is the paramagnetic center, equations (5) and (6) become

$$\frac{1}{T_{1M}} = \frac{2}{15}\left(\frac{\mu_0}{4\pi}\right)^2 \gamma_H^2\gamma_S^2\hbar^2 S(S+1)\frac{1}{r^6} \times\left[\frac{7\tau_{c2}}{1+(\omega_S\tau_{c2})^2} + \frac{3\tau_{c1}}{1+(\omega_H\tau_{c1})^2}\right] \quad (10)$$

$$\frac{1}{T_{2M}} = \frac{1}{15}\left(\frac{\mu_0}{4\pi}\right)^2 \gamma_H^2\gamma_S^2\hbar^2 S(S+1)\frac{1}{r^6} \times\left[4\tau_{c1} + \frac{13\tau_{c2}}{1+(\omega_S\tau_{c2})^2} + \frac{3\tau_{c1}}{1+(\omega_H\tau_{c1})^2}\right] \quad (11)$$

where $\hbar$ is the Planck constant.

In the magnetic field range used in MRI, the main parameters governing the efficacy of a paramagnetic Gd-complex are q, τ_R, and τ_M. For low molecular weight complexes, r_1 and r_2 are comparable.

4.1.2 Second-sphere Mechanism

This contribution concerns the water molecules that are not directly coordinated to the paramagnetic ions and organized into a second coordination sphere (Figure 2).

The Solomon–Bloembergen–Morgan theory can be applied to SS water molecules. If $\Delta\omega_M \leq 1/{\tau_M}^{SS}$ and $1/{T_{2M}}^{SS}$, R_i^{SS} can described as

$$R_1^{SS} = fq^{SS}\frac{1}{{T_{1M}}^{SS} + {\tau_M}^{SS}} \quad (12)$$

$$R_2^{SS} = fq^{SS}\frac{1}{{T_{2M}}^{SS} + {\tau_M}^{SS}} \quad (13)$$

where q^{ss} is the number of water molecules in the second coordination sphere and ${\tau_M}^{SS}$ is the water residence time of these water molecules, which is much shorter than τ_M. For Gd-complexes,

$$\frac{1}{{T_{1M}}^{SS}} = \frac{2}{15}\left(\frac{\mu_0}{4\pi}\right)^2 \gamma_H^2\gamma_S^2\hbar^2 S(S+1)\frac{1}{{r_{SS}}^6} \times\left[\frac{7{\tau_{c2}}^{SS}}{1+(\omega_S{\tau_{c2}}^{SS})^2} + \frac{3{\tau_{c1}}^{SS}}{1+(\omega_H{\tau_{c1}}^{SS})^2}\right] \quad (14)$$

$$\frac{1}{{T_{2M}}^{SS}} = \frac{1}{15}\left(\frac{\mu_0}{4\pi}\right)^2 \gamma_H^2\gamma_S^2\hbar^2 S(S+1)\frac{1}{{r_{SS}}^6} \times\left[4{\tau_{C1}}^{SS} + \frac{13{\tau_{c2}}^{SS}}{1+(\omega_S{\tau_{c2}}^{SS})^2} + \frac{3{\tau_{c1}}^{SS}}{1+(\omega_H{\tau_{c1}}^{SS})^2}\right] \quad (15)$$

where r_{SS} is the distance between the SS water protons and the unpaired electron spins, and ${\tau_{c1,2}}^{SS}$ are the correlation times modulating the interaction, with

$$\frac{1}{{\tau_{ci}}^{SS}} = \frac{1}{\tau_R} + \frac{1}{\tau_M^{SS}} + \frac{1}{\tau_{si}} \quad (16)$$

4.1.3 Outer-sphere Mechanism

OS relaxation has been described by Freed as that resulting from the long-distance dipolar interaction between the spin of the paramagnetic compound and the nuclear spin (Figure 2). The mechanism is modulated by the translational correlation time (τ_D) that takes into account the relative diffusion constant (D) of the ion center and of the solvent molecule and their distance of closest approach (d). The OS contribution is given by equations (17–20):

$$R_1^{OS} = \frac{6400\pi}{81}\left(\frac{\mu_0}{4\pi}\right)^2 \gamma_H^2\gamma_S^2\hbar^2 S(S+1)NA\frac{[C]}{dD} \times[7j(\omega_S\tau_D) + 3j(\omega_H\tau_D)] \quad (17)$$

$$R_2^{OS} = \frac{6400\pi}{81}\left(\frac{\mu_0}{4\pi}\right)^2 \gamma_H^2\gamma_S^2\hbar^2 S(S+1)NA\frac{[C]}{dD} \times[6.5j(\omega_S\tau_D) + 1.5j(\omega_H\tau_D) + 2j(0)] \quad (18)$$

$$\tau_D = \frac{d^2}{D} \quad (19)$$

$$j(\omega\tau_D) = \mathrm{Re}\left[\frac{1 + \frac{1}{4}(i\omega\tau_D + \tau_D/\tau_{S1})^{1/2}}{1 + (i\omega\tau_D + \tau_D/\tau_{S1})^{1/2} + \frac{4}{9}(i\omega\tau_D + \tau_D/\tau_{S1}) + \frac{1}{9}(i\omega\tau_D + \tau_D/\tau_{S1})^{3/2}}\right] \quad (20)$$

For low molecular weight Gd-complexes with one coordinated water molecule, this contribution is similar to the IS contribution. However, contrary to the IS contribution, the OS contribution is quite insensitive to the size of the complex. As a result, the OS contribution of large Gd-complexes becomes very small as compared to the IS one.

4.1.4 NMRD Profiles of Paramagnetic Gd-complexes

The evolution of the paramagnetic relaxation as a function of the magnetic field (nuclear magnetic relaxation dispersion profile or (NMRD) profile) is a powerful tool to approach some of the numerous parameters describing the IS, SS, and OS contributions (11 parameters: τ_M, q, τ_R, τ_V, τ_{s0}, r, ${\tau_M}^{SS}$, q^{SS}, r_{ss}, D, and d). Considering the large number of parameters, the estimation of all of them by the field cycling technique is often ambiguous. Thus, the determination of some parameters by independent methods like ^2H or ^{17}O NMR facilitates the theoretical adjustment of the NMRD curve. It is worth noting that the OS mechanism always contributes to the relaxivity,

eMagRes, Online © 2007 John Wiley & Sons, Ltd.

This article was previously published in the *Encyclopedia of Magnetic Resonance* in 2009 by John Wiley & Sons, Ltd.
DOI: 10.1002/9780470034590.emrstm1049

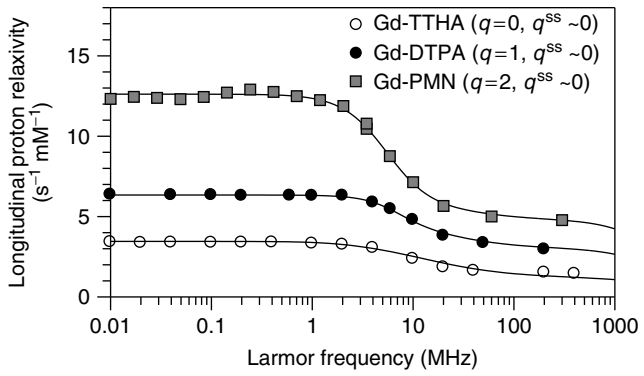

Figure 3 NMRD profiles at 310 K of three different linear complexes of Gd^{3+}: Gd-TTHA (triethylenetetraamine hexaacetic acid gadolinium chelate) for which only the OS contribution is observed ($q = 0$), Gd-DTPA (diethylenetriamine pentaacetic acid gadolinium chelate) with one water molecule in the first coordination sphere of Gd^{3+}, and Gd-PMN ([2,6-pyridinediylbis(methylene nitrilo] tetraacetic acid gadolinium chelate) tetraacetate with two water molecules in the first coordination sphere of Gd^{3+}

whereas the IS and the SS contributions are present only if one or more water molecules exchanging with the bulk are found in the first or in the second coordination sphere (Figure 3).

4.2 Superparamagnetic Relaxation

4.2.1 Mechanisms

Magnetite (Fe_3O_4) and maghemite (γ-Fe_2O_3) are two important ferrimagnetic iron oxides that are known to exhibit extremely high magnetic moments due to cooperative alignment of the electronic spins of the individual paramagnetic ions. These ferrites are characterized by high saturation magnetization at 300 K (92 emu g^{-1} for magnetite and 78 emu g^{-1} for maghemite).[7]

In superparamagnetic colloids, the IS relaxation mechanism does not contribute significantly to the proton relaxation, which occurs because of the fluctuations of the dipolar magnetic coupling between the nanocrystal magnetization and the proton spin. The relaxation is described by an OS model where the dipolar interaction fluctuates because of both the translational diffusion process and the Néel relaxation process (which can be compared to the electronic relaxation of a paramagnetic ion). However, the classical OS theory as such is not applicable to these particles. A model has been proposed[8,9] (Figure 4) that fits the NMRD experimental data and allows predictions of the size and the saturation magnetization.

4.2.2 NMRD Profiles of Superparamagnetic Nanoparticles

At low fields (Figure 4), the longitudinal relaxation rate of the protons is obtained by introducing in the OS equations the limitation of the precession: the electron Larmor precession frequency is set to zero. The spectral density function determining this component of the relaxation is then characterized by a global correlation time depending on τ_N and τ_D, which are, respectively, the Néel relaxation time and the translation correlation time.

At high fields (Figure 4), the magnetic vector is locked along the external field B_o, and the Curie relaxation dominates. The corresponding relaxation rates are given by an OS model assuming a stationary magnetization component in the B_o direction and, therefore, an infinite value of the Néel relaxation time. The dispersion of this spectral density (named the *Ayant function*) occurs when $\omega_H.\tau_D \sim 1$.

At intermediate fields (Figure 4), the relaxation rates are combinations of the high-field and low-field contributions, weighted by factors depending on the Langevin function that gives the average magnetization of the sample.

4.3 Susceptibility-Induced Relaxation

The mechanisms presented so far describe the enhancement of the relaxation processes due to short-range interactions between the water protons and the magnetic centers. In addition, microscopic magnetic field gradients created by susceptibility differences between compartments can be responsible for another type of relaxation enhancement that concerns only the transverse evolution of the nuclear magnetization. High concentrations of paramagnetic or superparamagnetic derivatives in the intravascular space induce an increase of the bulk susceptibility of this compartment and, hence, a decrease of

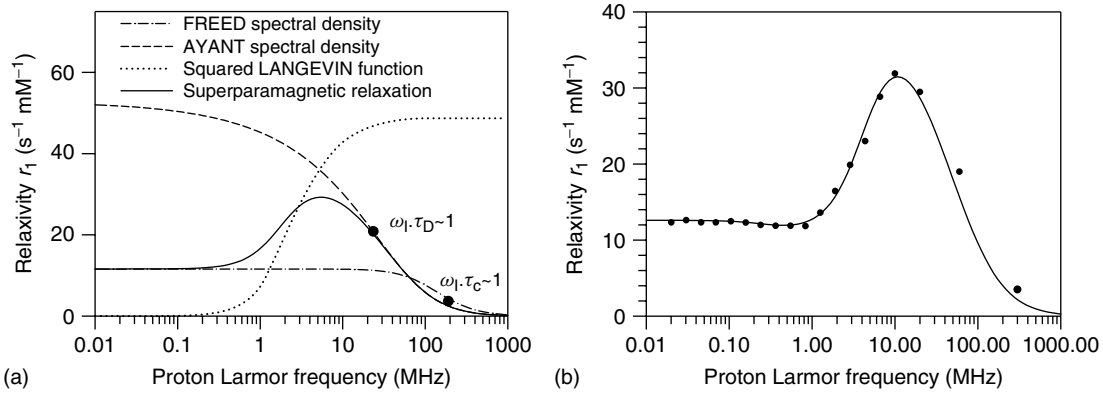

Figure 4 Illustration of the superparamagnetic model (T = 310 K, $d = 10$ nm, $M_s = 40.8$ Am^2 (kg ferrite)$^{-1}$, $\tau_N = 1.8$ ns) (a) and NMRD curve of nanoparticles obtained by coprecipitation of $FeCl_2$ and $FeCl_3$ in the presence of dextran ($d = 8.62$ nm, $Ms = 59.5$ Am^2 (kg ferrite)$^{-1}$, τ_N 0.9 ns) (b)

eMagRes, Online © 2007 John Wiley & Sons, Ltd.

This article was previously published in the *Encyclopedia of Magnetic Resonance* in 2009 by John Wiley & Sons, Ltd.
DOI: 10.1002/9780470034590.emrstm1049

the apparent transverse relaxation time T_2^* due to the water diffusion through the transcompartmental magnetic field heterogeneities. This phenomenon will be maximal in gradient echo imaging sequences that do not contain spin refocusing radiofrequency pulses able to minimize this irreversible loss of phase coherence. Pure susceptibility effects are only achievable with magnetic materials exhibiting negligible r_1. Among such susceptibility agents are those paramagnetic ions and complexes that have very short electronic relaxation times $\tau_{s1,2}$, for example, dysprosium(III).

5 CONTRAST AGENTS

5.1 Paramagnetic Contrast Agents

To increase the efficacy of T_1-shortening paramagnetic contrast agents, several parameters can, in principle, be optimized: the hydration number q of the metal ion, the residence time of the coordinated water τ_M, the rotational correlation time τ_R, and the metal proton distance r.

q: the larger the value of q is, the better the efficacy of the contrast agent will be (Figure 3). However, the in vivo stability of Gd-complexes with large q values remains problematic.

τ_M: the mechanism of IS relaxation is based on an exchange between bulk water molecules surrounding the complex and the water molecule(s) coordinated to the lanthanide. Consequently, the exchange rate ($k_{ex} = 1/\tau_M$) is an essential parameter for transmitting the "relaxing" effect to the solvent. This parameter has been studied in large series of complexes in order to understand the important factors.[10] Its measurement is based on the works of Swift and Connick for diluted paramagnetic solutions and consists of an analysis of the ^{17}O transverse relaxation rate.[11]

For low molecular weight complexes, τ_M values lower than 500 ns do not limit the relaxivity in the MRI field range at 310 K. On the contrary, for larger complexes, smaller values of τ_M (<40 ns) are needed in order to avoid a quenching of the relaxing effect.

τ_R: several methods have been proposed to lengthen τ_R: enzyme-catalyzed oligomerization, noncovalent interactions with endogenous macromolecules like human seric albumin (HSA), DNA, specific receptors of the cellular membrane, paramagnetic polymers, liposomes, or micelles (see below). Large values of τ_R induce a maximum of the longitudinal relaxivity around 0.5–1.5 T, with a sharp decrease at magnetic fields larger than 2 T. On the contrary, the transverse relaxivity, which is similar to r_1 below 0.5 T, remains at a high value above 0.5 T (Figure 5).

r: in theory, a small decrease of r allows a quite large increase in relaxivity because of the $1/r^6$ dependence of T_{1M}. However, this distance is nearly constant in all stable Gd-complexes ($r = 0.31 \pm 0.01$ nm) already described.

Currently, several low molecular weight compounds are used in clinical applications (Figure 6; Table 1).[12] Among them, Gd-DTPA, (diethylenetriaminepentaacetate gadolinium chelate) Gd-DTPA-BMA, (diethylenetriaminepentaacetate-bis (methylamide) gadolinium chelate) Gd-DOTA, (tetraazacyclododecanetetraacetic acid gadolinium chelate), and Gd-HP-DO3A (hydroxypropyl-tetraazacyclododecanetriaacetic acid gadolinium chelate) were the first to be used clinically.

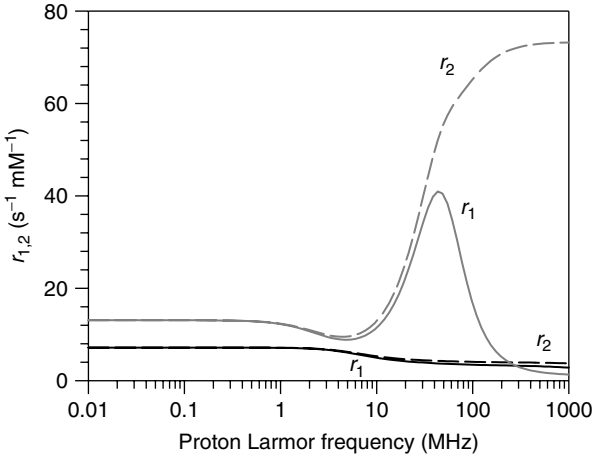

Figure 5 Simulation of proton NMRD relaxivities for Gd-complexes with $q = 1$, $r = 0.31$ nm, $\tau_M = 100$ ns, $\tau_{sO} = 100$ ps, $\tau_V = 20$ ps, and $\tau_R = 60$ ps (black lines) or $\tau_R = 6$ ns (gray lines). The OS contribution was calculated with $d = 0.36$ nm and $D = 3\ 10^{-9}\ m^2\ s^{-1}$

In vivo, they have an extravascular and extracellular distribution and a fast renal excretion.

Gd-EOB-DTPA (ethoxybenzyl-diethylenetriaminepentaacetic acid gadolinium chelate) is a lipophilic complex that enters the hepatocytes and allows for the detection of hepatic lesions characterized by a decrease (nonhepatocellular metastases) or an increase (hepatocellular carcinoma) of the hepatocytes signals.

Two types of blood pool agents can be found: serum albumin binding Gd chelates and high molecular weight compounds with long blood circulation times. MS-325 belongs to the first category: by binding to serum albumin, its relaxivity is increased and its residence time in the blood is prolonged. In the second category, one can find P-792 (Vistarem®, Guerbet, France), which is a large compound, although based on a low molecular weight contrast agent. This macromolecular blood pool contrast agent that has high relaxivity (Figure 7) and a slow extravasation is small enough to be quickly and completely eliminated by glomerular filtration.

Necrosis-avid contrast agents (NACAs), useful for the detection of necrosis in the context of pathologies such as myocardial infarction, have been proposed. Within these agents, we find both porphyrin [e.g., Gadophrin-2 (bis-gadolinium mesoporphyrins from Bayer Schering Pharma AG)] and nonporphyrin species (e.g., ECIV-7 and ECIII-60).

All the Gd chelates described above contain only one Gd^{3+} ion. To achieve the high relaxivity values needed for molecular MRI, several types of molecular carriers, able to bring high Gd concentrations to the target site, have been built. Proteins (albumin, avidin, and polylysine) or dendrimers have been conjugated to Gd chelates in order to carry a large number of metal atoms. Gadomer-17 (Bayer Schering Pharma AG) is made of a dendrimer. The 24 free amino groups are linked to a macrocyclic DOTA gadolinium chelate, allowing for the complexation of 24 Gd atoms. To improve their selective delivery, molecular carriers must be conjugated to ligands specific for a given target (receptors, overexpressed molecules specific of a pathology, antibodies, or antibody fragments). In the case of avidin-Gd-DTPA complexes, avidin induces the binding of the contrast agent to the target after its prelabeling

eMagRes, Online © 2007 John Wiley & Sons, Ltd.

This article was previously published in the *Encyclopedia of Magnetic Resonance* in 2009 by John Wiley & Sons, Ltd.
DOI: 10.1002/9780470034590.emrstm1049

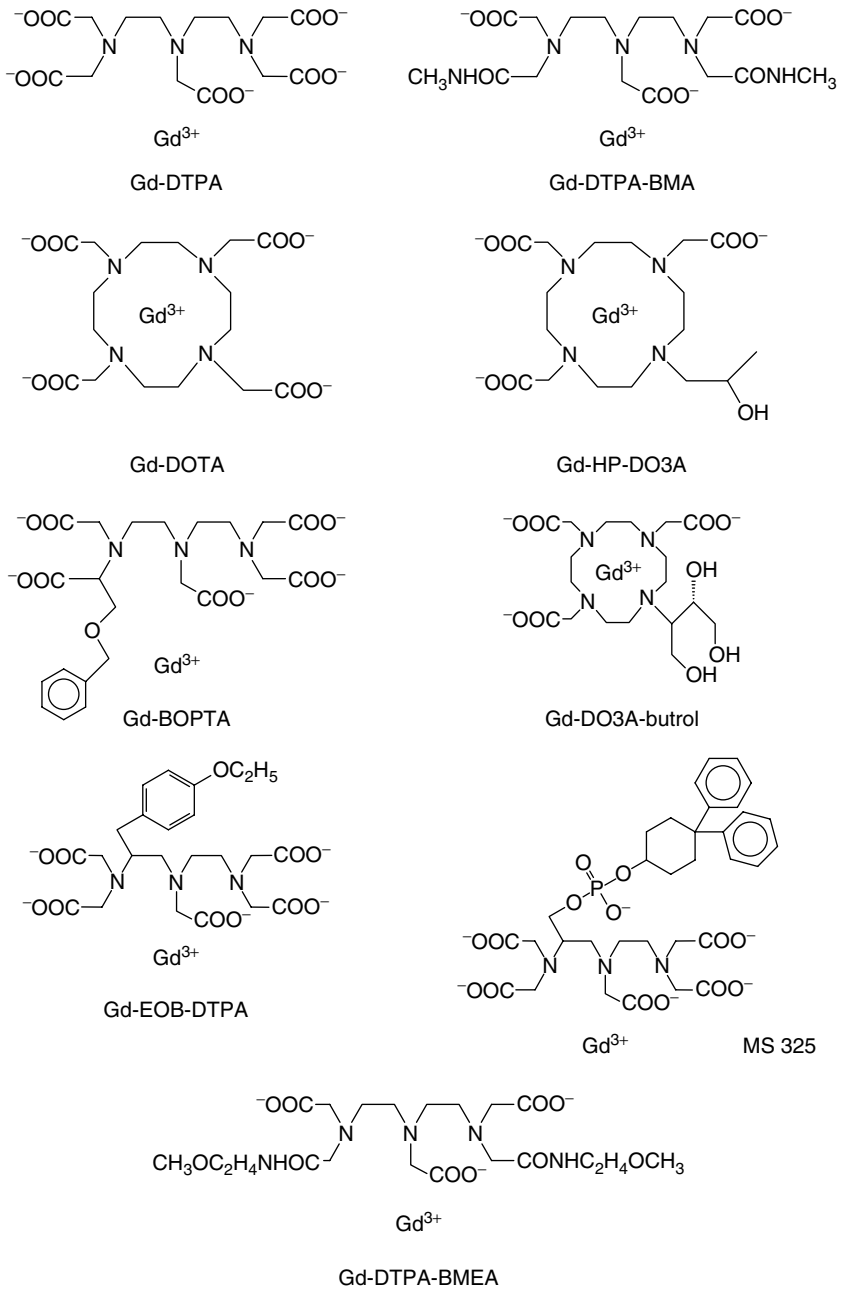

Figure 6 Chemical structure of commercial and clinical Gd-complexes

with a biotinylated antibody. This Gd carrier has been used to image tumor cells expressing the HER-2/*neu* receptor-1 in an animal model of breast cancer. The avidin–biotin system was also used to link biotinylated Gd-perfluorocarbon nanoparticles to a biotinylated antibody specific for an endothelial integrin characteristic of angiogenic vessels, $\alpha_v\beta_3$, in order to image neovessels in an animal model of angiogenesis.

Liposomes loaded with a molar concentration of Gd also provide a high T_1 relaxivity. Paramagnetic liposomes conjugated to a specific antibody have made it possible to image endothelial cells expressing an inflammatory surface molecule [ICAM-1(intercellular adhesion molecule 1)] in an animal model of brain inflammation. Another inflammatory marker expressed by endothelial cells, E-selectin, has been imaged using a polylysine-based Gd carrier linked to a specific antibody fragment in vitro. Gd chelates have been directly conjugated to an antibody or to a synthetic mimetic of the natural ligand of E-selectin (the sialyl-Lewis^x molecule) in order to target, respectively, human melanoma xenografts or inflamed endothelial cells in vivo.

5.2 Superparamagnetic Contrast Agents (Iron Oxide Nanoparticles: USPIO and SPIO)

There are three kinds of particulate magnetic contrast agents: ultrasmall particles of iron oxide (USPIO), with a hydrodynamic diameter between 10 and 40 nm; small particles

eMagRes, Online © 2007 John Wiley & Sons, Ltd.

This article was previously published in the *Encyclopedia of Magnetic Resonance* in 2009 by John Wiley & Sons, Ltd.
DOI: 10.1002/9780470034590.emrstm1049

Table 1 Examples of commercial or clinical Gd-complexes

Contrast agent	Name	Company	Relaxivity (s^{-1} mM^{-1}) At 60 MHz, 310 K
Gd-DTPA	Magnevist, gadopentetate dimeglumine	Bayer Schering Pharma AG, Germany	3.3
Gd-DTPA-BMA	Omniscan, Gadodiamide	General Electric Healthcare, UK	3.3
Gd-DOTA	Dotarem, gadoterate meglumine	Guerbet, France	2.9
Gd-HP-DO3A	Prohance, Gadoteridol	Bracco, Italy	2.9
Gd-BOPTA	MultiHance, gadobenate dimeglumine	Bracco, Italy	4.0
Gd-DO3A-butrol	Gadovist, Gadobutrol	Bayer Schering Pharma AG, Germany	3.3
Gd-EOB-DTPA	Primovist, Eovist	Bayer Schering Pharma AG, Germany	5.4
Gd-DTPA-BMEA	Gadoversetamide, Optimark	General Electric Healthcare, UK	3.8
MS-325	Vasovist	Bayer Schering Pharma AG	5.4

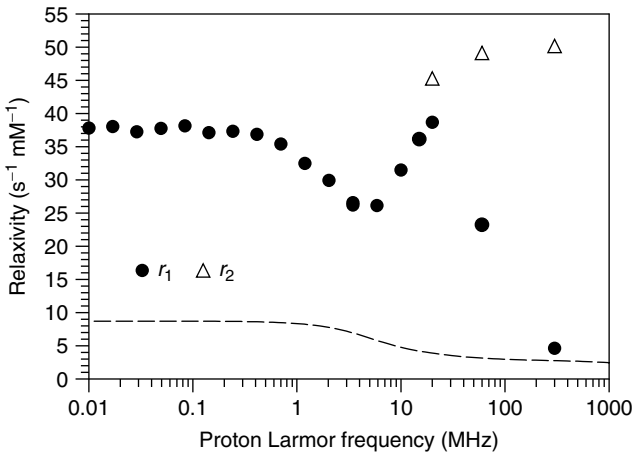

Figure 7 Proton NMRD data of P-792 obtained at 310 K. The proton NMRD profile of DOTA-Gd (dashed line) has been added for comparison

of iron oxide (SPIO), with a hydrodynamic diameter between 60 and 150 nm; and oral (large) particles, with a hydrodynamic diameter between 300 nm and 3.5 µm. Two subcategories of USPIO are called *monocrystalline iron oxide nanoparticles* (*MIONs*) (hydrodynamic diameter between 10 and 30 nm) and crosslinked iron oxide (CLIO) (hydrodynamic diameter between 10 and 30 nm), a form of MION with cross-linked dextran coating. Particles of submicrometer size can be used by intravenous administration. Some particles have been approved for clinical application or are being clinically tested (Table 2).[4,5,7]

The efficacy as well as the stability of the nanoparticles depends on several parameters, such as the size of the iron oxide crystal, their hydrodynamic size, charge, coating, etc. The chemical coating of the particles allows to link vectors able to target a specific area as an organ or a particular biological system, or to label cells.

A number of processes have been adapted to produce magnetic nanoparticles from solution, aerosol, or vapor phase. After synthesis, a coating is required to prevent agglomeration and to prepare a stable colloidal suspension in aqueous and biological media (Table 3). For example, Massart's method for rapid synthesis of γ-Fe_2O_3 particles has allowed coating with various small molecules like amino acids, α-hydroxyacids (citric, gluconic, etc.), or dimercaptosuccinic acid. Polymeric compounds have also been used, including polysaccharides (dextran and derivatives, arabinogalactan), organic siloxanes, polyethylene glycol (PEG), etc. A typical example of polymeric stabilization is the synthesis of ferumoxide by the Molday coprecipitation method with in situ dextran coating.

5.3 CEST, PARACEST, and LIPOCEST Contrast Agents

Additional contrast agents involving chemical exchange-based mechanism called *chemical exchange saturation transfer* (*CEST*) are currently investigated. Besides intrinsic metabolites that can be imaged on the basis of their water proton exchange rates using saturation transfer techniques, exogenous molecules exhibiting a chemical exchange-dependent saturation transfer with bulk water molecules under physiological conditions can be used. These agents reduce the bulk water proton signal through a chemical exchange site on the agent via saturation transfer. Numerous candidate chemicals (amino acids, sugars, nucleotides, and heterocyclic ring chemicals) have been evaluated but their chemical shift is quite limited. Theory predicts that the ideal chemical exchange site should have a large chemical shift from water and a slow exchange at physiological pH (6.5–7.6) and a temperature of 310 K. Some paramagnetic complexes [Eu(III), Dy(III), Pr(III), Nd(III), and Tb(III) complexes] with proton sites (H_2O, −NH, and −OH) shifted far away from the bulk water resonance and exchanging slowly enough ($k_{ex} \leq \Delta\omega$) have been proposed and are now referred to as *paramagnetic chemical exchange saturation transfer* (*PARACEST*) *agents*.[13] A new class of CEST contrast agents, called *liposome chemical exchange saturation transfer* (*LIPOCEST*) *agents*, is based on liposomes encapsulating shift agents. In such nanosized systems, the resonance frequency of the water protons located inside the liposomes is different from the extraliposomal water. By controlling the water permeability of the liposomal membrane, it is possible to increase their CEST effect.[14]

eMagRes, Online © 2007 John Wiley & Sons, Ltd.

This article was previously published in the *Encyclopedia of Magnetic Resonance* in 2009 by John Wiley & Sons, Ltd.
DOI: 10.1002/9780470034590.emrstm1049

Table 2 Examples of commercial USPIO and SPIO agents

Contrast agent	Name	Company	Particle size	Target organs
AMI-25	Ferumoxide Endorem Feridex IV	Guerbet, Berlex Laboratories	80–150 nm	R_2 enhanced in normal RES cells of the liver/spleen
AMI-227	Ferumoxtran Sinerem Combidex	Guerbet, Advanced Magnetics	20–40 nm	R_2 enhanced in normal RES cells of the liver/spleen/lymph/bone marrow R_1 enhancement observed in highly blood-perfused tissue at early stages
SHU 555A	Resovist Ferucarbotran	Bayer Schering Pharma AG,	62 nm	R_2 enhanced in normal RES cells of the liver/spleen R_1 enhancement observed in highly blood-perfused tissue at early stages
NC100150	Clariscan	General Electric Healthcare	20 nm	R_2 enhanced in normal RES cells of the liver/spleen R_1 enhancement observed in highly blood-perfused tissue at early stages
AMI-121	Ferumoxil Lumirem Gastromark	Guerbet, Advanced Magnetics	300 nm	R_2 enhanced in gastrointestinal system
OMP	Abdoscan	General Electric Healthcare	3.5 μm	R_2 enhanced in gastro-intestinal system

Table 3 Examples of coating materials and biological applications[5]

Coating molecules	Applications
Citric acid	Cellular targeting
Silane	Silane coupling agents for molecular imaging targeting
Dextran	Long plasma half-life
Polyethylene glycol (PEG)	Long plasma half-life, improves the biocompatibility
Polyvinyl alcohol (PVA)	Long plasma half-life, drug delivery, tendon repair
Polypeptides	Cell biology, targeting cells
Poly (D, L-lactide)	Biocompatible, low cytotoxicity
Polyvinylpyrrolidone (PVP)	Long plasma half-life
Chitosan	Nonviral gene delivery system, biocompatible
Polymethylmethacrylate (PMMA)	Drug delivery
Polyethyleneimine (PEI)	Gene vectors

6 SOME APPLICATIONS OF MRI CONTRAST AGENTS

Smart contrast agents sensitive to pH, calcium, or enzyme have been developed. For example, the q number of a relaxometric probe can be sensitive to the intra or extracellular pH. As a result, the IS relaxivity will change. The use of a removable group that is not coordinated to the paramagnetic ion, but excludes water molecules from the coordination sphere because of its sterical hindrance, results in a relaxivity increase in the presence of a cleavage agent, for example, enzymatic cleavage with β-galactosidase.[15] Recently, there has also been increased interest in the application of iron oxide nanoparticles to cell targeting.[16]

E-selectin is found on the cell surface of endothelial cells. It binds to sialyl-Lewis^x (a carbohydrate moiety) on the cell surface of leukocytes. Tumor necrosis factor α (TNFα) and interleukin-1 (IL-1), released from inflammatory stimuli, upregulate E-selectin and other adhesion molecule expression on the vascular endothelial cells, which leads to leukocyte adhesion to the activated endothelium. A sialyl-Lewis^x mimetic was conjugated to USPIO nanoparticles for noninvasive MRI of E-selectin expression on activated endothelial cells. These nanoparticles were successfully tested in a mouse model of hepatitis. MRI results obtained with this contrast agent suggested that the nanoparticles uptake by macrophages was attenuated by an interaction between the sialyl-Lewis^x mimetic and the endothelial E-selectin.[17]

Apoptosis is a physiological process that may become pathologic either by overactivity or inhibition. A dedicated

eMagRes, Online © 2007 John Wiley & Sons, Ltd.

This article was previously published in the *Encyclopedia of Magnetic Resonance* in 2009 by John Wiley & Sons, Ltd.
DOI: 10.1002/9780470034590.emrstm1049

contrast agent evidencing pathologies where apoptosis takes place is useful for early diagnosis and to monitor therapies. Phage display technology has been used to select a peptide with high affinity for phosphatidylserine (PS), a marker of apoptosis. Subsequent coupling of this linear hexapeptide with USPIO has produced a selective MRI contrast agent whose efficacy has been tested on Jurkat cells culture.[18]

7 CONCLUSIONS AND PERSPECTIVES

In the development of new MRI contrast agents, particular attention is paid to their molecular structure with the aim of optimizing their physicochemical and biological properties.

The physicochemical analyses include proton relaxometric profile, magnetometry, and photon correlation spectroscopy for superparamagnetic particles, on one hand, and, on the other hand, proton relaxometric profile, water residence time of the coordinated water molecule, stability versus transmetallation, and interaction with serum proteins for paramagnetic complexes.

Contrast agents designed for molecular imaging must target pathology. Therefore, a specific vector is needed to ensure the specific interaction of the contrast agent with the pathological cells. These vectors can be chosen from the peptides selected by phage display or among the nonpeptide mimetics proposed in the literature.

The "contrastophore" (paramagnetic or superparamagnetic) in a molecularly targeted contrast agent should be characterized by a high relaxivity and magnetic susceptibility in order to be easily detectable by NMR in low concentrations and it should be conjugated to the vector molecule (ligand specific for the targeted receptor) with no loss of the specific affinity. MRI offers the advantage of being noninvasive and furnishing simultaneously and with a high spatial resolution anatomical, physiological, and molecular information. Nevertheless, the quite low sensitivity of MRI contrast agents represent a challenge that can be met either by design of better agents or by the development of improved NMR protocols for their detection.

To enhance the relaxivity of paramagnetic contrast agents, their physicochemical properties must be optimized in order to reduce their rotational mobility and the residence time of the coordinated water molecules. The relaxivity of superparamagnetic contrast agents is considerably larger since each crystal contains several thousand paramagnetic ions, while paramagnetic compounds frequently contain only one ion per molecule. Consequently, the superparamagnetic particles appear as more efficient for molecular imaging, but the negative contrast they produce on MR images makes them less convenient for in vivo diagnosis.

8 RELATED ARTICLES

Contrast Agents in Magnetic Resonance: Operating Mechanisms; Contrast Agents in MRI: Superparamagnetic Iron Oxide; Contrast Agents in Whole Body Magnetic Resonance: An Overview; Gadolinium Chelate Contrast Agents in MRI: Clinical Applications; Gadolinium Chelates: Chemistry, Safety and Behavior; Magnetic Resonance Imaging: A Historical Overview; Magnetization Transfer Contrast: Clinical Applications; Paramagnetic Relaxation in Solution; Relaxation: An Introduction; Relaxation Measurements in Imaging Studies; Relaxation Measurements in Whole Body MRI: Clinical Utility.

9 REFERENCES

1. P. A. Rinck, ed, *Magnetic Resonance in Medicine*, 4th, Completely Revised Edition, Blackwell Wissenschafts–Verlag: Berlin, 2001.
2. K. W.-Y. Chan and W.-T. Wong, *Coord. Chem. Rev.*, 2007, **251**, 2428.
3. B. Yoo and M. D. Pagel, *Front. Biosci.*, 2008, **13**, 1733.
4. P. Majewski and B. Thierry, *Crit. Rev. Sol. State Mater. Sci.*, 2007, **32**, 203.
5. S. Laurent, D. Forge, M. Port, A. Roch, C. Robic, L. Vander Elst, and R. N. Muller, *Chem. Rev.*, 2008, **108**(6), 2064.
6. J. Kowalewski, Paramagnetic relaxation in solution, in *Encyclopedia of Nuclear Magnetic Resonance*, eds, D. M. Grant and R. K. Harris, John Wiley & Sons: New York, 1996, 3456.
7. A. K. Gupta and M. Gupta, *Biomaterials*, 2005, **26**, 1563.
8. A. Roch, R. N. Muller, and P. Gillis, *J. Chem. Phys.*, 1999, **110**, 5403.
9. A. Roch, R. N. Muller, and P. Gillis, *J. Magn. Reson. Imaging*, 2001, **14**, 94.
10. A. E. Merbach and E. Toth, ed, *The Chemistry of Contrast Agents in Medical Magnetic Resonance Imaging*, John Wiley & Sons: Chichester, 2001.
11. D. H. Powell, O. M. Ni Dhubhghaill, D. Pubanz, Y. Lebedev, W. Schlaepfer, and A. E. Merbach, *J. Am. Chem. Soc.*, 1996, **118**, 9333.
12. H.-J. Weinmann, A. Mühler, and B. Radüchel, Gadolinium chelates: chemistry, safety and behavior, in *Encyclopedia of Nuclear Magnetic Resonance*, eds, D. M. Grant and R. K. Harris, John Wiley & Sons: New York, DOI: 10.1002/9780470034590.emrstm0183.
13. M. Woods, D. E. Woessner, and A. D. Sherry, *Chem. Soc. Rev.*, 2006, **35**, 500.
14. S. Aime, S. Geninatti Crich, E. Gianolio, G. B. Giovenzana, L. Tei, and E. Terreno, *Coord. Chem. Rev.*, 2006, **250**, 1562.
15. L. Frullano and T. J. Meade, *J. Biol. Inorg. Chem.*, 2007, **12**, 939.
16. J. W. M. Bulte and M. M. J. Modo, *Nanoparticles in Biomedical Imaging, Emerging Technologies and Applications*, Springer: New York, 2007.
17. S. Boutry, S. Laurent, L. Vander Elst, and R. N. Muller, *Contrast Media Mol. Imaging*, 2006, **1**(1), 15.
18. C. Laumonier, J. Segers, S. Laurent, A. Michel, L. Vander Elst, and R. N. Muller, Selecting vectors to image apoptosis by phage display technique, *21th Annual Meeting of the European Society for Magnetic Resonance in Medicine and Biology, 2004, Copenhagen, Denmark*.

Acknowledgments

The authors thank Mrs Patricia de Francisco for her help in preparing the article. This work was supported by the FNRS and the ARC Program 05/10-335 of the French Community of Belgium. The support and sponsorship concerted by COST Action D38 and EMIL Program are kindly acknowledged.

DOI: 10.1002/9780470034590.emrstm1049

Biographical Sketches

Sophie Laurent. *b.* 1967. M.Sc., 1989, Ph.D., 1993 in Chemistry. Currently lecturer at University of Mons-Hainaut (Belgium). Leader of the chemical synthesis team of the General, Organic and Biomedical Chemistry Laboratory. Author of more than 65 original papers. Present research interest: synthesis and vectorization of contrast agents for molecular imaging.

Luce Vander Elst. *b.* 1955. M.Sc., 1978, Ph.D. 1984 in Chemistry. Postdoctoral research: Multinuclear NMR analysis of the metabolism of perfused hearts, Medical School of Harvard University 1986. Professor at the University of Mons-Hainaut, Belgium. Author of more than 95 original papers. Research interests: high resolution NMR and physicochemical characterization of MRI contrast agents.

Robert N. Muller. *b.* 1948. M.Sc., 1969, Ph.D. 1974 in Chemistry, Full Professor, University of Mons-Hainaut, Belgium. Member of Paul C. Lauterbur's research group at the State University of New York at Stony Brook in 1981–1982. Sabbatical with Prof. Ivano Bertini, University of Florence, Italy (2002–2003). Author of more than 130 original papers and 6 books. Head of the Department of General, Organic and Biomedical Chemistry.

eMagRes, Online © 2007 John Wiley & Sons, Ltd.

This article was previously published in the *Encyclopedia of Magnetic Resonance* in 2009 by John Wiley & Sons, Ltd.
DOI: 10.1002/9780470034590.emrstm1049